UDC 539.31/.53:661.878

Junyu Li[1], Jianling Zhao[2], Cuiming Tang[3, *], Peng Chen[1], Shiquan Feng[1, **]

[1]College of Physics and Electronic Engineering,
Zhengzhou University of Light Industry, Zhengzhou, China
[2]Division of Radiation Physics, State Key Laboratory of Biotherapy and Cancer Center, West China Hospital, Sichuan University, Chengdu, China
[3]Department of Physics and Electronic Engineering,
Sichuan University of Science & Engineering, Zigong, China
**49273185@163.com*
***2014079@zzuli.edu.cn*

Theoretical investigation on the elastic properties, bond stiffness and hardness of WX_2 (X = B and N)

In this paper, we investigate the elastic properties, bond stiffness, hardness and Debye temperatures for hexagonal $P6_3/mmc$ WX_2 (X = B or N). It is observed that these two compounds are stable in mechanics. Both these two have three typical bonds, W–X bonds, X–X and W–W bonds. By investigating the bond stiffness of these three types of bonds, we found that the bulk modulus of WX_2 is mainly determined by W–X and W–W bonds, while the shear modulus is mainly determined by X–X bonds. In addition, using a theoretical model, we evaluate the hardness of these two compounds. Results showed that the Vickers hardness of WN_2 is much lower than that of WB_2. What's more, by calculating the Debye temperatures, we found the melting point of WN_2 is much lower than WB_2, and the overall chemical bonds in WB_2 are stronger than that of WN_2.

***Keywords**: superhard materials, elastic properties, bond stiffness, hardness, Debye temperatures.*

INTRODUCTION

As an important research direction of superhard materials in the future, transition-metal borides have advantages of easy synthesis and low cost. So, great progress has been made in investigating this type of materials.

Chung et al. [1, 2] synthesized ultra-incompressible transition-metal boride, ReB_2, by arc melting at ambient pressure. Further research showed that rhenium diboride (ReB_2) is an ultrahard material with a hardness of approximately 48 GPa under a load of 0.49 N, and it was thought to be currently the hardest known transition metal diboride. But this research caused a substantial controversy. Dubrovinskaia et al. [3] figured out that ReB_2 is not a superhard material, because the load invariant hardness of it is below 30 GPa. But as a response, Chung et al. [4] provided an atomic force microscopy profile of scratch marks of ReB_2 on the diamond surface. Up to now, it is still debated on whether ReB_2 is a superhard material. Compared with ReB_2, it is no doubt that RuB_2, OsB_2 and WB_2 are not superhard

materials [5–8]. But tungsten, as one of the few transition metals, is known for its ability to form higher boron content borides, and tungsten borides have much more advantages compared to other transition-metal borides: (i) tungsten is relatively inexpensive, (ii) tungsten is one of the few transition metals which can form higher boron content borides. To find more boron-rich structures, Ma et al. [9] used a systematic first-principles global structural optimization method to search the structures of tungsten borides. They established for the first time the thermodynamically stable structures for boron-rich tungsten borides hexagonal $P6_3/mmc$-2u W_2B_5 and hexagonal R-3m-6u WB_3. As two new predicted phases of boron-rich tungsten borides, there are few reports on their physical properties. In our previous study, we have systematically explored the structural, elastic and electronic properties for these two transition-metal borides WB_x(x = 2.5, 3.0) [10].

But the hardness of tungsten borides is not ideal, it limits the application of this kind of materials. Therefore, studying the factors influencing hardness and exploring the method to improve hardness has important scientific significance in the design of transition metal boride superhard materials. Studies show that pressure, cation doping and anion doping can change the hardness of transition metal borides. In our previous study, we investigated the structural stability, electronic properties and hardness for three Re-doped hexagonal W_2B_5 compounds to explore the influence of Re-doping structural regulation on hardness characteristics. In addition, we also studied the hardness and other properties of W_2B_5 at high pressure [11]. But there are few studies on the effect of of anion doping on hardness of transition metal borides. In this work, we intend to investigate the elastic properties, bond stiffness, hardness and Debye temperatures for hexagonal $P6_3/mmc$ ReB_2–WX_2 (X = B or N). This work would provide a theoretical basis for improving the hardness of transition metal borides by anion doping.

COMPUTATIONAL METHODS AND DETAILS

In this letter, the structural, electronic properties, bond stiffness and hardness of WX_2 (X = B and N) are investigated by standard Kohn-Sham self-consistent density functional theory [12–13]. The atoms positions are optimized by using the conjugate gradient (CG) algorithm, and the self-consistency tolerance is set to 1×10^{-6} eV for the total energy per atom and 0.001 eV/Å for atomic force in the structural optimization. For the exchange-correlation energy, the generalized gradient approximation designed by Perdew, Burke, and Ernzerhof (PBE) [14–15] is used in the calculation. Pseudopotentials plane-wave method is adopted to describe the valence electron interaction with the atomic core. The valence electronic configurations for W, B and N are set as $5s^25p^6$ $5d^46s^2$, $2s^22p^1$ and $2s^22p^3$, respectively. A plane-wave basis set with an energy cutoff of 450 eV is closed to ensure a stable state of the system energy. The 5×5×2 k-points in the Brillouin zone is performed using Monkhorst-pack grid [16].

RESULTS AND DISCUSSIONS

Structural Stability and Elastic properties

Previous lots of investigations of diborides show the measured Vickers hardness of ReB_2 is larger than other diborides like MB_2 (M = Os, W, Ta and Ru) [5–8]. It is due to its special structure. In this paper, we use the first principles calculations to investigate hexagonal $P6_3/mmc$ ReB_2–WX_2 (X = B or N). The structure is presented as following Fig. 1. Our calculated theoretical lattice parameters are a = b = 2.927 Å, c = 7.735 Å with W at Wyckoff 2c (0.33333, 0.66667, 0.25) and B at

4*f* (0.33333, 0.66667, 0.540638) positions for WB_2; and $a = b = 3.100$ Å, $c = 7.255$ Å with W at Wyckoff 2*c* (0.33333, 0.66667, 0.25) and B at 4*f* (0.33333, 0.66667, 0.601559) positions for WN_2. Our calculated results are good agreement with theoretical work of Ma et al. [9].

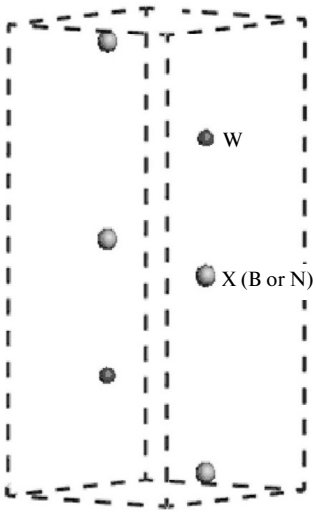

Fig. 1. The crystal structure of hexagonal $P6_3/mmc$ ReB_2–WX_2 (X = B or N).

To investigate the mechanical stability of WX_2 (X = B or N), we calculated the elastic constants of them by the strain-stress method, and judge whether they are stable by the generalized elastic stability criteria.

For hexagonal phase, the mechanical stability criteria are as follows:

$$C_{44} > 0,\ C_{11} > |C_{12}|,\ (C_{11} + 2C_{12})C_{33} > 2C_{13}. \tag{1}$$

The bulk modulus *B*, shear modulus *G* and Young's modulus *E* can be calculated via the Voigt-Reuss-Hill (VRH) approximations:

$$B_v = \frac{1}{9}\left[2(C_{11} + C_{12}) + 4C_{13} + C_{33}\right]; \tag{2}$$

$$G_V = \frac{1}{30}(C_{11} + C_{12} + 2C_{33} - 4C_{13} + 12C_{44} + 12C_{66}); \tag{3}$$

$$B_R = \frac{(C_{11} + C_{12})C_{33} - 2C_{13}^2}{C_{11} + C_{12} + 2C_{33} - 4C_{13}}; \tag{4}$$

$$G_R = \frac{\frac{5}{2}\left[(C_{11} + C_{12})C_{33} - 2C_{13}^2\right]C_{44}C_{66}}{3B_V C_{44}C_{66} + \left[(C_{11} + C_{12})C_{33} - 2C_{13}^2\right](C_{44} + C_{66})}, \tag{5}$$

where B_V and G_V are the bulk and shear modulus in the Voigt scheme, respectively; B_R and G_R are the bulk and shear modulus in the Reuss scheme, respectively [17].

According to the VRH approximations [18], the bulk modulus *B*, shear modulus *G* and Young's modulus *E* of a polycrystalline material can be calculated by following formulas:

$$B = \frac{1}{2}(B_R + B_V),\ G = \frac{1}{2}(G_R + G_V); \tag{6}$$

$$E = \frac{9BG}{3B + G}. \tag{7}$$

Table 1. The elastic constants, GPa, of hexagonal phase WB_2 and WN_2

	C_{11}	C_{12}	C_{13}	C_{33}	C_{44}	B_V	G_V	B_R	G_R
WB_2	592.4	169.3	93.2	950.0	260.2	316.3	265.0	308.6	252.2
WN_2	482.4	258.9	168.4	296.7	114.3	272.5	112.4	246.9	110.1

In Table 2, we listed the B, G, E and B/G for hexagonal phase WB_2 and WN_2. It can be seen that the bulk modulus B, shear modulus G and Young's modulus E for WB_2 are much larger than the counterpart of WN_2. In order to explore the reasons, we need to further study the bond components of the two structures.

Table 2. The *B*, *G*, *E*, GPa, and *B*/*G* for hexagonal phase WB_2 and WN_2

	B	*G*	*E*	*B*/*G*
WB_2	312.4	258.6	608.0	1.208
	320.0 [7]	208.0 [7], 273.0 [19]		
WN_2	259.7	111.3	292.1	2.333

Bond Stiffness

Bai et al. proposed a simple model to characterize the bond stiffness [20–21]. According to this model, they can obtain the bond stiffness k by fitting a quadratic curve to the relative bond lengths d/d_0 (d_0 is the bond length at 0 GPa) as a function of p. The pressure dependence of relative bond lengths can be expressed as a form of polynomial function ($d/d_0 = C_0 + C_1p + C_2p^2$) (where p is the hydrostatic pressure, C_i (i = 0, 1, 2) are the quadratic fitting coefficients). And then the bond stiffness k can be computed by following formula:

$$k = \left|\frac{d(d/d_0)}{dp}\right|^{-1} = \left|C_1 + 2C_2p\right|^{-1}. \tag{8}$$

Using the above theoretical model, we obtained the relationship of the normalized bond length of WB_2 and WN_2 changed as pressure and gave them in following Fig. 2, *a* and Fig. 3, *a*, respectively. By fitting the pressure dependence of relative bond lengths to polynomial function, we calculated the quadratic fitting coefficients for different bonds. And then the bond stiffness can be calculated formula (8). In Figs. 2, *b* and 3, *b*, we depicted the bond stiffness as a function of p for WB_2 and WN_2, respectively.

In the structure of WX_2 (X = B or N), there are three types of bonds: W–X bonds, X–X bonds and W–W bonds. For WB_2, W–W bonds possess the highest stiffness (1244.7 GPa), while weakest bond stiffness is B–B bonds (970.9 GPa). But for WN_2, W–N bonds possess the highest stiffness (1916.1 GPa), while weakest bond stiffness is N–N bonds (418.4 GPa). The bond stiffness of compounds has an important influence on the elastic properties. In this study, by analyzing the results of bulk/shear modulus and bond stiffness of WX_2 (X = B or N), we can

guess that the bulk modulus of WX_2 is mainly determined by W–X and W–W bonds, and the shear modulus is mainly determined by X–X bonds.

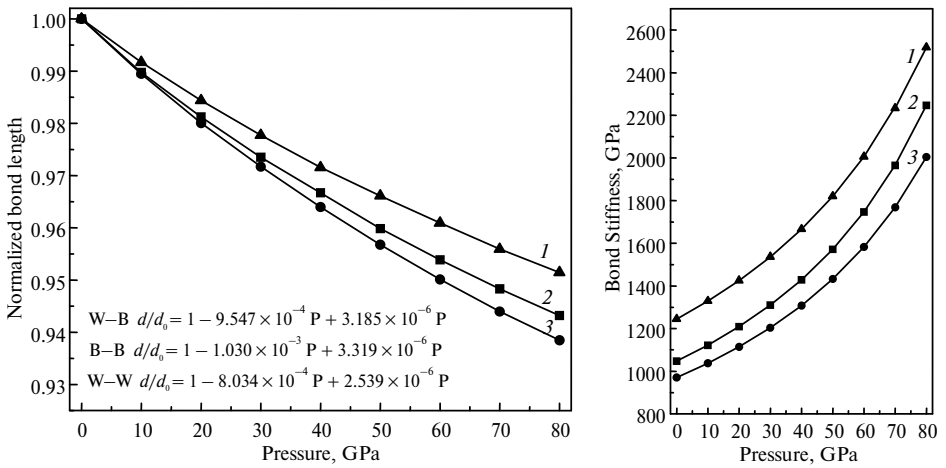

Fig. 2. The normalized bond length changed as pressures p (*a*) and the bond stiffness as a function of p (*b*) for WB_2: W–W (*1*), W–B (*2*), B–B (*3*).

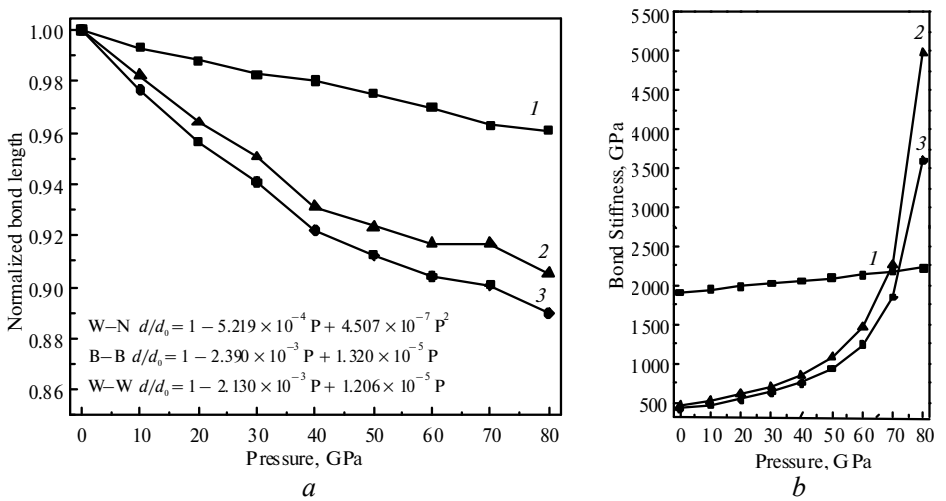

Fig. 3. The normalized bond length changed as pressures p (*a*) and the bond stiffness as a function of p (*b*) for WN_2: W–N (*1*), W–W (*2*), N–N (*3*).

Table 3. The bond stiffness, GPa, for WX_2 (X = B or N) at zero pressure.

Bond	W–X	X–X	W–W
WB_2	1047.4	970.9	1244.7
WN_2	1916.1	418.4	469.5

Although the highest bond stiffness (W–W bonds) in WB_2 is much smaller than the highest bond stiffness (W–N bonds) of in WN_2, the bulk modulus of WB_2 is a little larger than that of WN_2 after a comprehensive consideration of the factors of the bond stiffness of W–B in WB_2 and the bond stiffness of W–W in WB_2. In addi-

tion, because the stiffness of B–B bonds in WB_2 is much stronger than the N–N bonds in WN_2, so the shear modulus of WB_2 is much higher than that of WN_2.

Hardness

Vicker's hardness is an important parameter to measure the abrasion performance of materials. In previous work [10, 22], we have studied the influence factor of the hardness of transition metal borides and phosphides. There are several theoretical models to calculate theoretical Vickers hardness. In this work, we use theoretical model proposed by Tian et al. [23] to calculate the hardness of WB_2 and WN_2. In this model, $H_V = 0.92\, k^{1.137} G^{0.708}$, where the $k = G/B$, B and G are the bulk modulus and shear modulus of crystals, respectively. Both bulk and shear moduli are macroscopic concepts.

Table 4 presents the calculated Vicker's hardness of WB_2 and WN_2, they are 37.9 and 9.9 GPa, respectively. This result is well agreement with the result obtained by Gao's model [24, 25]. it can be seen that the hardness of WN_2 is much smaller than that of WB_2 and is mainly limited by the shear modulus G. Above, we discussed the relationship of the bond stiffness and bulk/shear modulus. Considering this, we can conclude that a small bond stiffness of N–N bonds leads to a low hardness for WN_2.

Table 4. The theoretical hardness of WX_2 (X = B or N)

	B, GPa	G, GPa	k	H_v, GPa
WB_2	312.4	258.6	0.828	37.9
				35.7 [24]
WN_2	259.7	111.3	0.429	9.9

Debye temperature

The Debye temperature is an important thermal quantity to predict thermodynamic properties such as the melting temperature of the material. According to the Debye model [26], the Debye temperature can be calculated from the average sound velocity of a polycrystalline material by the following formula:

$$\theta_{\mathrm{D}} = \frac{h}{k_{\mathrm{B}}}\left[\frac{3n}{4\pi}\left(\frac{N_{\mathrm{A}}\rho}{M}\right)\right]^{\frac{1}{3}} v_a, \tag{11}$$

where h is the Plank's constant, k_{B} is the Boltzmann's constant, N_{A} is Avogadro's number, ρ is the mass density, M is the molecular weight, and n is the number of atoms in the molecule, v_a is the average sound velocity of a material. While the average sound velocity can be obtained from the transverse (v_t) and longitudinal (v_l) sound velocities by following formula:

$$v_a = \left[\frac{1}{3}\left(\frac{2}{v_t^3} + \frac{1}{v_l^3}\right)\right]^{-\frac{1}{3}}. \tag{12}$$

While the longitudinal and transverse sound velocities can be computed from the shear and bulk moduli, and the mass density ρ from the following formula:

$$v_t = \left(\frac{3B + 4G}{3\rho}\right)^{\frac{1}{2}}; \tag{13}$$

$$v_t = \left(\frac{G}{\rho}\right)^{\frac{1}{2}}. \quad (14)$$

According to above theoretical formulas, we calculated the Debye temperature of WB_2 and WN_2 and listed them in following Table 5.

Table 5. Calculated Debye temperature of WB_2 and WN_2

Compounds	v_l, m/s	v_t, m/s	v_a, m/s	ρ, g/cm^3	θ_D, K
WB_2	2347.7	1472.7	1621.7	11.93	227.5
WN_2	1853.5	968.0	1082.9	11.88	149.3

Different materials have the different Debye temperatures. The higher the Debye temperature, the higher the melting point, and the stronger the chemical bonds between the atoms. So the melting point of WB_2 is higher than WN_2. And the overall chemical bonds in WB_2 are stronger than that of WN_2.

CONCLUSIONS

In this paper, the elastic constants, bond stiffness, hardness and Debye temperature of hexagonal $P6_3/mmc$ WX_2 (X = B or N) were studied by first principles theory. According to the calculated results of elastic constants, we further discussed the bulk modulus B, shear modulus G and Young's modulus E for WX_2 (X = B or N), and found that these moduli for WB_2 are much larger than their counterparts for WN_2. In order to explore the reasons, we studied the bond components and their bond stiffness for these two structures. Results showed that the bulk modulus of WX_2 is mainly determined by W–X and W–W bonds, and the shear modulus is mainly determined by X–X bonds. Although the highest bond stiffness in WB_2 is much smaller than the highest bond stiffness of in WN_2. Due to the comprehensive influences of W–W and W–X bonds, the bulk modulus of WB_2 is a little larger than that of WN_2. For the stiffness of B–B bonds much stronger than the N–N bonds, so the shear modulus of WB_2 is much higher than WN_2.In addition, by calculating the theoretical Vickers hardness of WX_2 (X = B or N), we found that a small bond stiffness of N–N bonds leads to a low hardness for WN_2. What's more, by analyzing the Debye temperature of WX_2 (X = B or N), we can see that the melting point of WB_2 is higher than WN_2 and the overall chemical bonds in WB_2 are stronger than that of WN_2. This work would provide a theoretical reference for improving the hardness of transition metal borides by anion doping.

FUNDING

Supported by the Key Research of Department Education of Henan Province (No. 17A140030), the cultivation project of young backbone teachers of Henan Province (2019GGJS137) and the Doctoral Fund of Zhengzhou University of Light Industry (2016XGGJS003).

Досліджено пружні властивості, жорсткість зв'язку, твердість і температура Дебая гексагональних ($P6_3/mmc$) сполук WX_2 (X = B або N). Спостерігається, що ці дві сполуки стійкі при механічній обробці. Обидва мають три типові зв'язки: W–X, X–X і W–W. При дослідженні жорсткості трьох типів зв'язків, виявлено, що об'ємний модуль WX_2 визначається в основному зв'язками W–X і W–W, тоді як модуль зсуву – зв'язками X–X. Крім того, використовуючи теоретичну модель, оцінено твердість цих двох сполук. Результати показали, що твердість по Віккерсу WN_2 значно нижча, ніж у WB_2. Більше того, за підрахунком температури Дебая, виявлено, що температура плав-

лення WN_2 набагато нижча, ніж WB_2, а загальні хімічні зв'язки в WB_2 сильніші, ніж у WN_2.

***Ключові слова**: надтверді матеріали, еластичні властивості, жорсткість зв'язки, твердість, температура Дебая.*

Исследованы упругие свойства, жесткость связи, твердость и температура Дебая для гексагональных ($P6_3/mmc$) соединений WX_2 (X = B или N). Замечено, что эти два соединения устойчивы при механичной обработке. Оба имеют три типичные связи: W–X, X–X и W–W. При исследовании жесткости этих трех типов связей, обнаружено, что объемный модуль WX_2 в основном определяется связями W–X и W–W, а модуль сдвига – связями X–X. Кроме того, используя теоретическую модель, оценили твердость этих двух соединений. Результаты показали, что твердость по Виккерсу у WN_2 намного ниже, чем у WB_2. Более того, вычисляя температуры Дебая, обнаружили, что температура плавления WN_2 намного ниже, чем у WB_2, а общие химические связи в WB_2 прочнее, чем у WN_2.

***Ключевые слова**: сверхтвердые материалы, упругие свойства, жесткость связи, твердость, температура Дебая.*

1. Chung H.-Y., Weinberger M.B., Levine J.B., Kavner A., Yang M., Tolbert S.H., Kaner R.B. Synthesis of ultra-incompressible superhard rhenium diboride at ambient pressure. *Science*. 2007. Vol. 316, no. 5823. P. 436–439.
2. Chung H.-Y., Weinberger M. B., Yang J.-M., Tolbert S.H., Kaner R.B. Correlation between hardness and elastic moduli of the ultraincompressible transition metal diborides RuB_2, OsB_2, and ReB_2. *Appl. Phys. Lett.* 2008. Vol. 92, no. 26. P. 261904.
3. Dubrovinskaia N., Dubrovinsky L., Solozhenko V.L. Comment on "synthesis of ultra-incompressible superhard rhenium diboride at ambient pressure". *Science*. 2007. Vol. 318, no. 5856. P.1550–1550.
4. Chung H.-Y., Weinberger M.B., Levine J.B., Cumberland R.W., Kavner A., Yang J.-M., Tolbert S.H., Kaner R.B. Response to ultra-incompressible superhard rhenium diboride at ambient of comment on "synthesis pressure". *Science*. 2007. Vol. 318, no. 5856. P.1550–1550.
5. Chiodo S., Gotsis H.J., Russo N., Sicilia E. OsB_2 and RuB_2, ultra-incompressible, hard materials: First-principles electronic structure calculations. *Chem. Phys. Lett*. 2006. Vol. 425, no. 4–6. P. 311–314.
6. Kiessling R. The crystal structures of molybdenum and tungsten borides. *Acta. Chem. Scand.* 1947. Vol. 1. P. 893-916.
7. Hao X.F., Xu Y., Wu Z., Zhou D., Liu X., Cao X., Meng J. Low-compressibility and hard materials ReB_2 and WB_2: Prediction from first-principles study. *Phys. Rev. B*. 2006. Vol. 74, no. 22, art. 224112.
8. Yang J., Sun H., Chen C.F. Is osmium diboride an ultra-hard material? *J. Am. Chem. Soc.* 2008. Vol. 130, no. 23. P. 7200–7201.
9. Li Q., Zhou D., Zheng W.T., Ma Y.M., Chen C.F. Global structural optimization of tungsten borides. *Phys. Rev. Lett.* 2013. Vol. 110, no. 13, art. 136403.
10. Feng S.Q., Guo F., Li J.Y., Wang Y.Q., Zhang L.M., Cheng X.L. Theoretical investigations of physical stability, electronic properties and hardness of transition-metal tungsten borides WB_x (x = 2.5, 3). *Chem. Phys. Lett.* 2015. Vol. 635. P. 205–209.
11. Feng S.Q., Yang Y., Li J.Y., Jiang X.X., Li H.N., Cheng X.L. Pressure effect on the hardness of diamond and W_2B_5: First-principle calculations. *Modern Physics Letters B*. 2017. Vol. 31, no. 12. P. 1750137.
12. Ordejón P., Artacho E., Soler J.M. Self-consistent order-N density-functional calculations for very large systems. *Phys. Rev. B*. 1996. Vol. 53, no. 16. P. R10441.
13. Strobel R., Maciejewski M., Pratsinis S.E., Baiker A. Unprecedented formation of metastable monoclinic $BaCO_3$ nanoparticles. *Therm. Acta.* 2006. Vol. 445, no. 1. P. 23–26.
14. Wu Z.G., Cohen R.E. More accurate generalized gradient approximation for solids. *Phys. Rev. B*. 2006. Vol. 73, no. 23, art. 2351161.
15. Perdew J.P., Burke K., Ernzerhof M. Generalized gradient approximation made simple. *Phys. Rev. Lett.* 1996. Vol. 77, no. 18. P. 3865.
16. Monkhorst H.J., Pack J.D. Special points for Brillouin-zone integrations. *Phys. Rev. B*. 1976. Vol. 13, no 12. P. 5188–5192.

17. Wu Z., Zhao E., Xiang H., Hao X., Liu X., Meng J. Crystal structures and elastic properties of superhard IrN_2 and IrN_3 from first principles. *Phys. Rev. B*. 2007. Vol. 76, no. 5, art. 054115.
18. Hill R. The elastic behaviour of a crystalline aggregate. *Proc. Soc. London. A*. 1952. Vol. 65. P. 349–349.
19. Chen X.Q., Fu C.L., Krčmar M., Painter G.S. Electronic and structural origin of ultraincompressibility of 5d transition-metal diborides MB_2 (M = W, Re, Os). *Phys. Rev. Lett.* 2008. Vol. 100, no. 19, art. 196403.
20. He X.D., Bai Y.L., Zhu C.C., Sun Y., Li M.W., Barsoum M.W. General trends in the structural, electronic and elastic properties of the M_3AlC_2 phases (M = transition metal): A first-principle study. *Comput. Mater. Sci.* 2010. Vol. 49, no. 3. P. 691–698.
21. He X. D., Bai Y. L., Zhu C. C., Barsoum M. W. Polymorphism of newly discovered Ti_4GaC_3: A first-principles study, *Acta Mater.* 2011. Vol. 59, no. 14. P. 5523–5533.
22. Feng S.Q., Li X.D., Su L., Li H.N., Yang H.Y., Cheng X.L. Ab initio study on structural, electronic properties, and hardness of re-doped W_2B_5. *Solid. Stat. Commun.* 2016. Vol. 245. P. 60–64.
23. Tian Y.J., Xu B., Zhao Z.S. Microscopic theory of hardness and design of novel superhard crystals. *Int. J. Refract. Met. H.* 2012. Vol. 33. P. 93–106.
24. Zhong M.M., Kuang X.Y., Wang Z.H., Shao P., Ding L.P., Huang X.F. Phase stability, physical properties, and hardness of transition-metal diborides MB_2 (M = Tc,W, Re, and Os): First-Principles Investigations. *J. Phys. Chem. C*. 2013. Vol. 117, no. 20. P. 10643–10652.
25. Gao F.M., He J.L., Wu E.D., Liu S.M., Yu D.L., Li D.C., Zhang S.Y., Tian Y.J. Hardness of covalent crystals. *Phys. Rev. Lett.* 2003. Vol. 91, no. 1, art. 015502.
26. Clarke D.R. Materials selection guidelines for low thermal conductivity thermal barrier coatings. *Surf. Coat Technol.* 2003. Vol. 163. P. 67–74.

Received 01.08.18
Revised 01.08.18
Accepted 04.10.18